Supporting Information

Fabrication of CdSe Nanosheet/CdS Nanorod Heterojunctions through Topotactic Transformation of Self-Template Photoanode for Enhanced Photoelectrochemical Hydrogen Production

Ruturaj P. Patil [a], Weon-Sik Chae [b], Hyun Gyu Kim[c], and Jum Suk Jang [*a]

[a]*Division of Biotechnology, College of Environmental and Bioresource Sciences, Jeonbuk National University, Iksan 570-752, Republic of Korea*

[b] *Daegu Center, Korea Basic Science Institute, Daegu 41566, Republic of Korea*

[c] *Busan Center, Korea Basic Science Institute (KBSI), Busan 46742, Republic of Korea*

*Corresponding authors

E-mail address: jangjs75@jbnu.ac.kr (Jum Suk Jang)

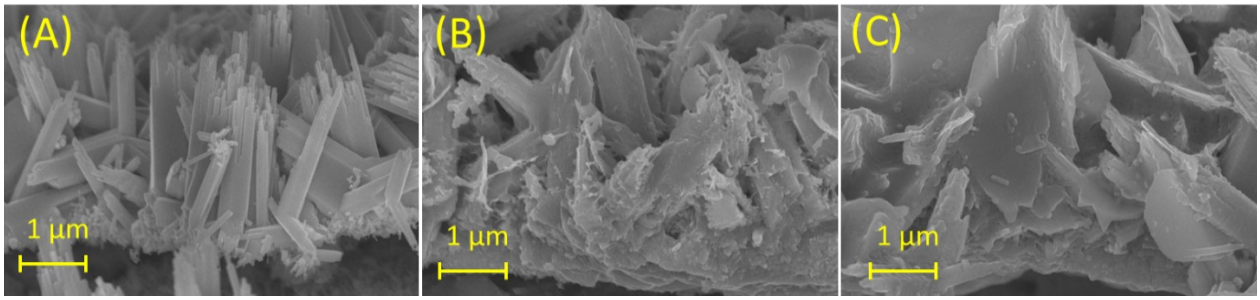

Fig. S1 Cross-section FE-SEM images of (A) CdSNR, (B) inorganic-organic $CdSe(en)_{0.5}NS/CdSNR$-3C, and (C) $CdSe(en)_{0.5}NS/CdSNR$-6C electrode, respectively.

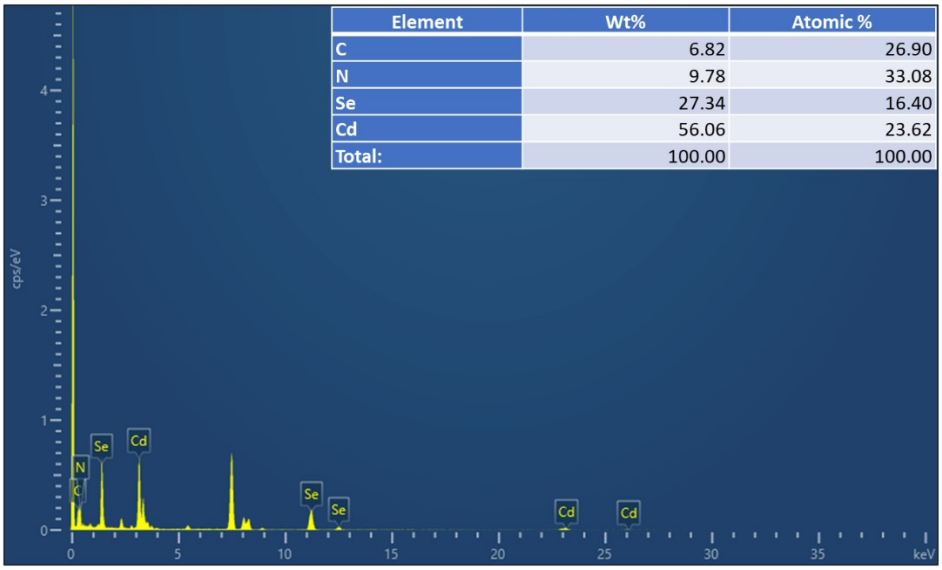

Fig. S2 EDS elemental spectrum and quantification results for inorganic-organic $CdSe(en)_{0.5}NS/CdSNR$ electrode ($CdSe(en)_{0.5}NS$).

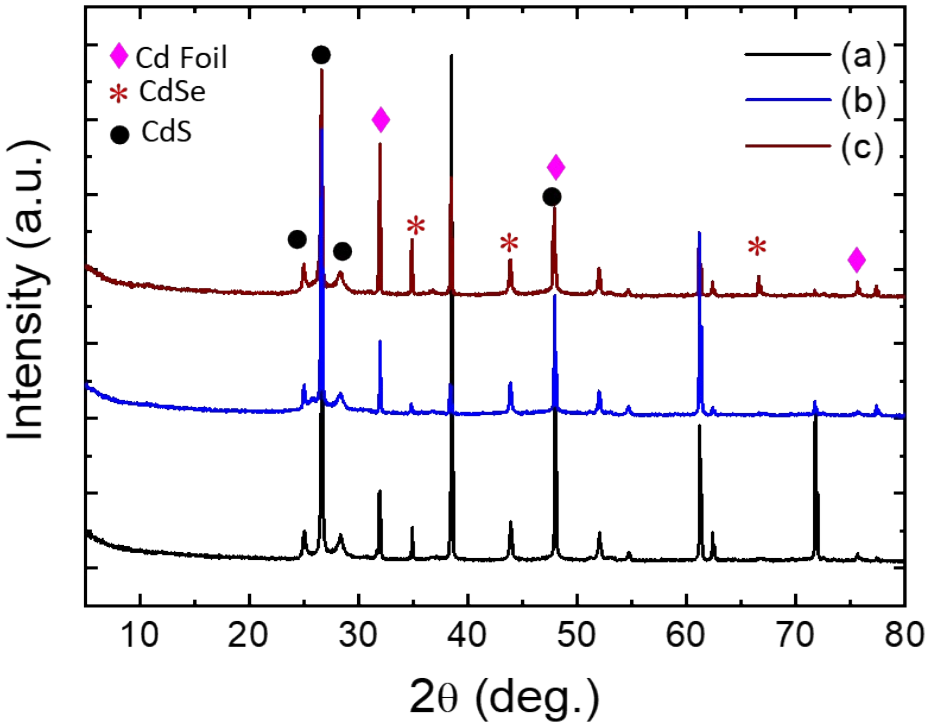

Fig. S3 XRD patterns of (a) CdSNR, (b) organic-organic $CdSe(en)_{0.5}NS/CdSNR$-3C, and (c) $CdSe(en)_{0.5}NS/CdSNR$-6C, respectively.

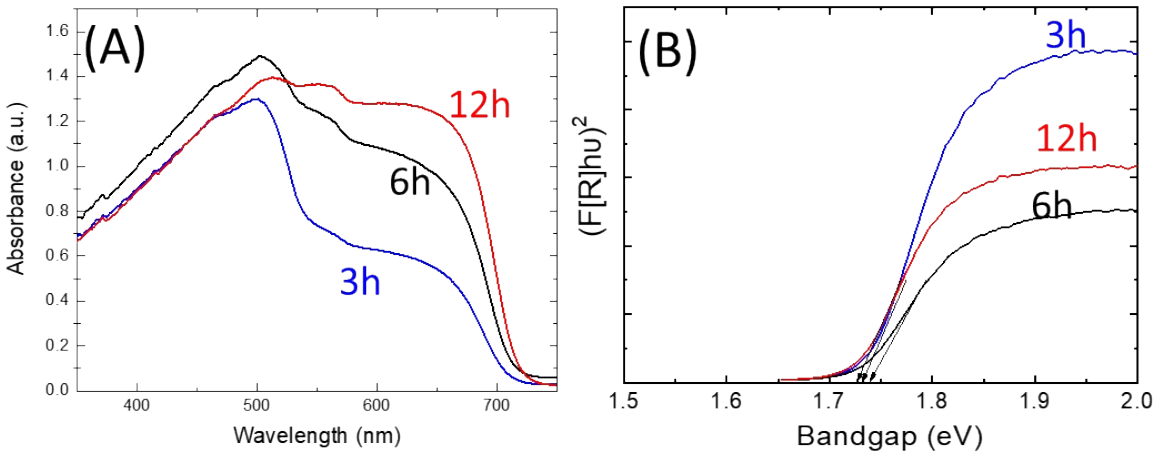

Fig. S4 (A, B) UV absorption spectra and bandgap for CdSeNS/CdSNR-3, CdSeNS/CdSNR-6, and CdSeNS/CdSNR-12 photoanodes.

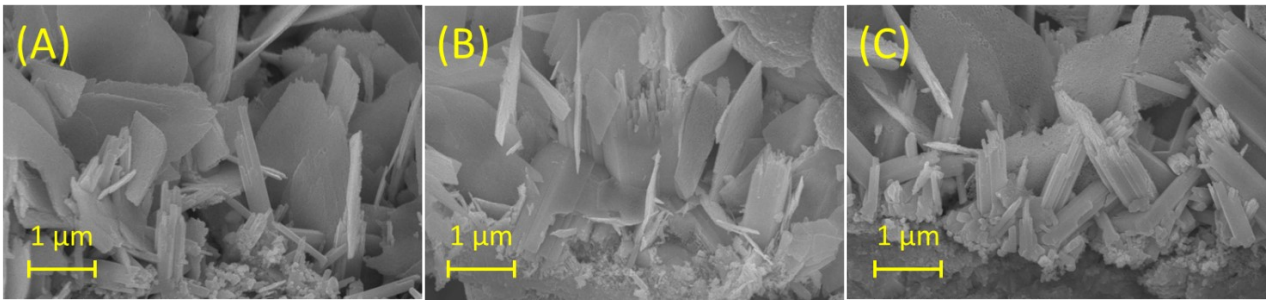

Fig. S5 Cross-section FESEM images of (A) CdSeNS/CdSNR-3 (B) CdSeNS/CdSNR-6, and (C) CdSeNS/CdSNR-12 photoanode, respectively.

Fig. S6 EDS elemental spectrum and quantification results for selective porous CdSeNS of CdSeNS/CdSNR-6h photoanode.

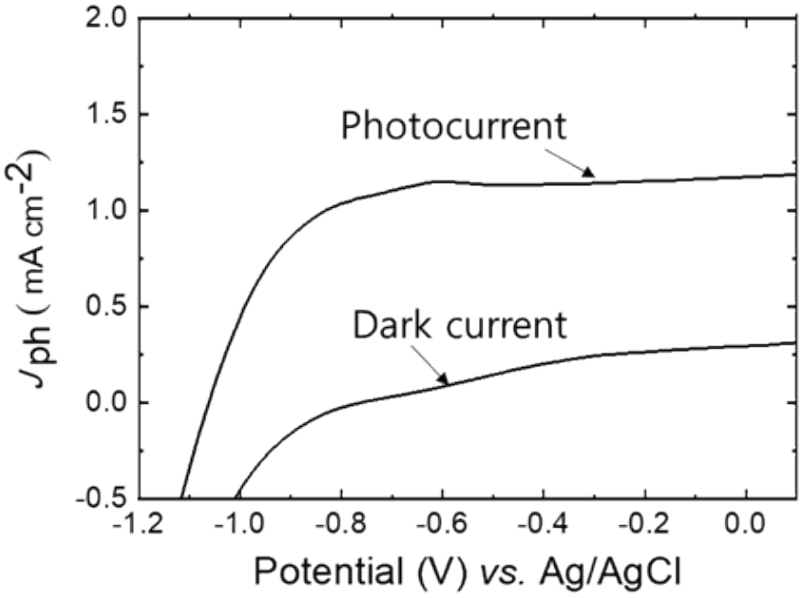

Fig. S7. Linear sweep voltammogram (J–V curve) of CdS NR (bare) photoanode.

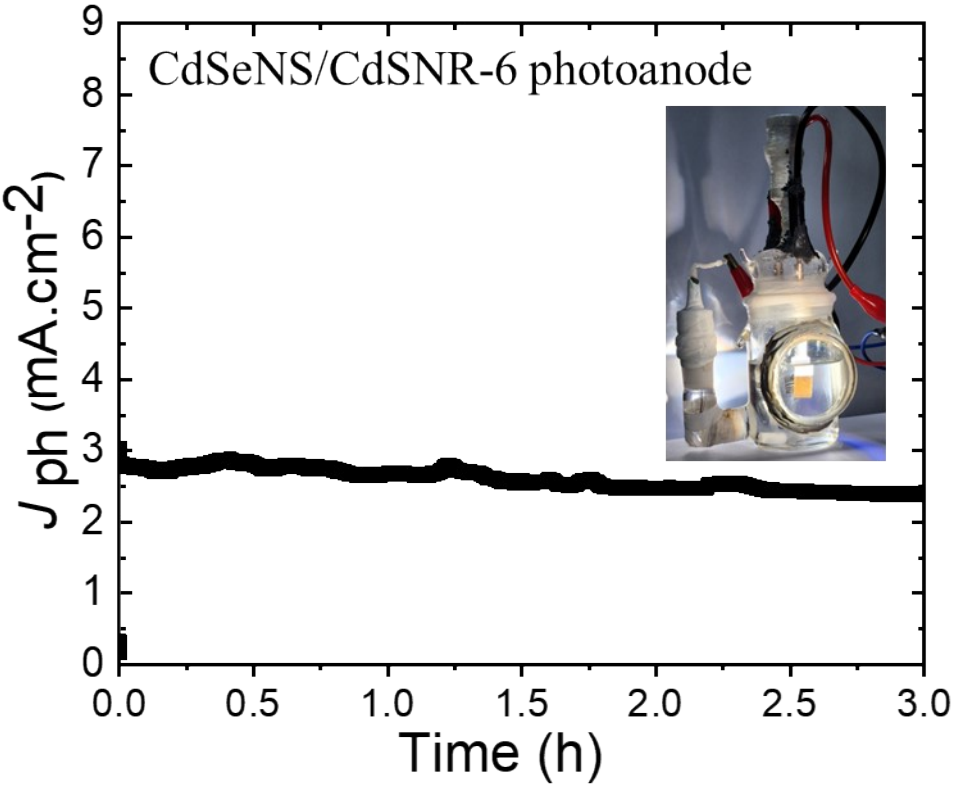

Fig. S8 Long-term stability of the CdSeNS/CdSNR-6 photoanode after the initial 3-hour hydrogen production run. The inset shows a digital photograph of the in-house custom-made photoelectrochemical (PEC) cell used for the measurement.

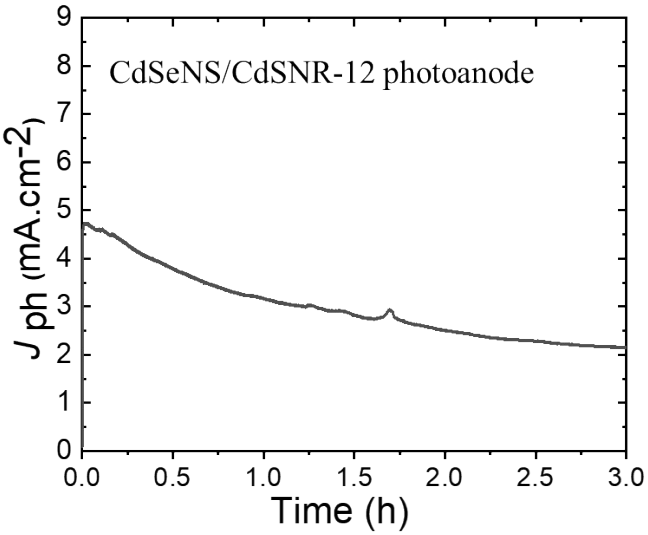

Fig. S9. Long-term stability of CdSeNS/CdSNR-12 photoanode.

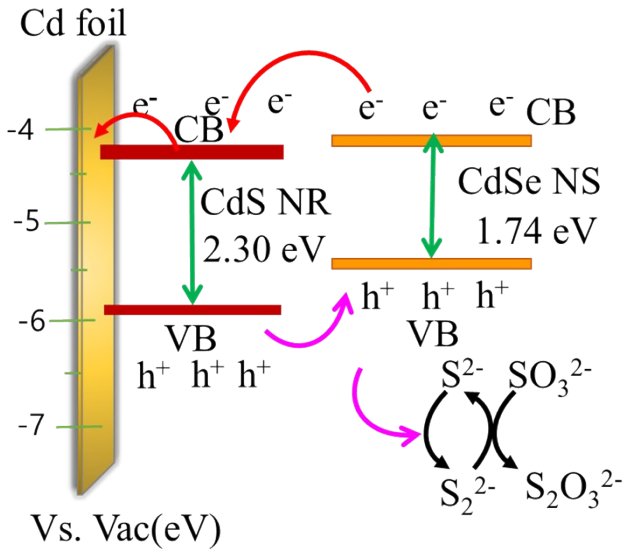

Fig. S10 Band alignment of CdSeNS/CdSNR heterojunction photoanode.

Photoelectrochemical hydrogen production mechanism over porous CdSeNS/CdSNR heterojunction photoanode

Under simulated solar illumination, CdSe absorbs photons and generates electron-hole pairs. The photogenerated electrons migrate to the Pt counter electrode where hydrogen evolution occurs, while the holes accumulate at the photoanode surface and react with sulfite (SO_3^{2-}) and sulfide (S^{2-}) ions in the electrolyte[1]: [2, 3]. □□□□□□□□□□□□□□□□□□□□□□□□□□□□

At Photoanode:

$$CdSeNS/CdSNR + h\upsilon \rightarrow CdSe\ (h^+ + e^-) \quad (1)$$

$$SO_3^{2-} + 2OH^- + 2\,h^+ \rightarrow SO_4^{2-} + 2H^+ \quad (2)$$

$$2S^{2-} + 2\,h^+ \rightarrow S_2^{2-} \quad (3)$$

$$S_2^{2-} + SO_3^{2-} \rightarrow S_2O_3^{2-} + S^{2-} \quad (4)$$

$$SO_3^{2-} + S^{2-} + 2h^+ \rightarrow S_2O_3^{2-} \quad (5)$$

At Pt electrode:

$$2H^+ + 2e^- \rightarrow H_2\uparrow \quad (6)$$

The instability of CdSeNS/CdSNR heterojunction photoanode in sulfide-containing electrolytes (Na_2S and Na_2SO_3) is well documented, and its degradation is exacerbated not only by excess surface-trapped photogenerated holes but also by the presence of dissolved oxygen, which accelerates photocorrosion. In contrast, Pt is chemically stable under these conditions and facilitates hydrogen evolution efficiently without degradation.

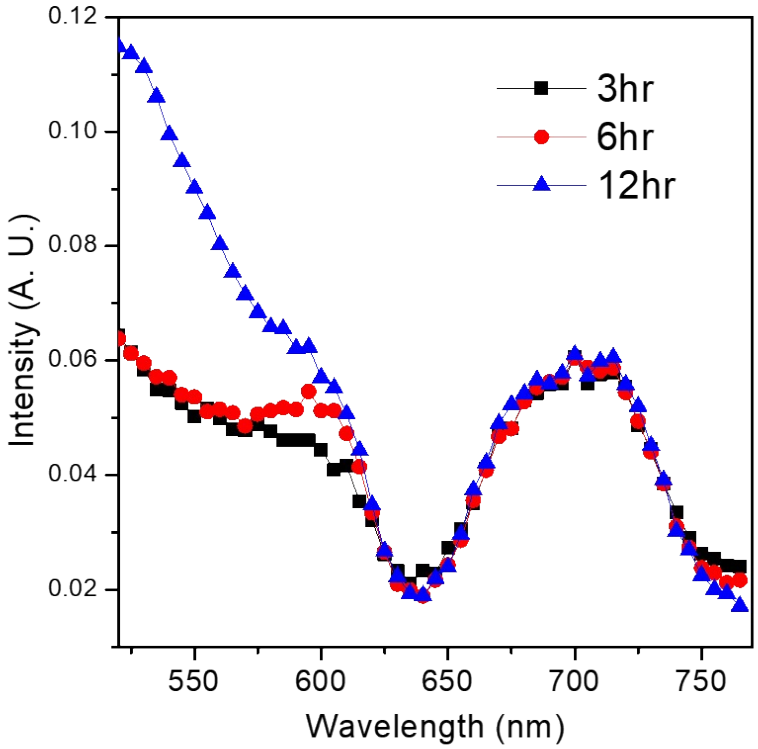

Fig. S11 Steady-state photoluminescence spectra of the CdSeNS/CdSNR photoelectrodes; 3 h (black square), 6 h (red circle), and 12 h (blue triangle).

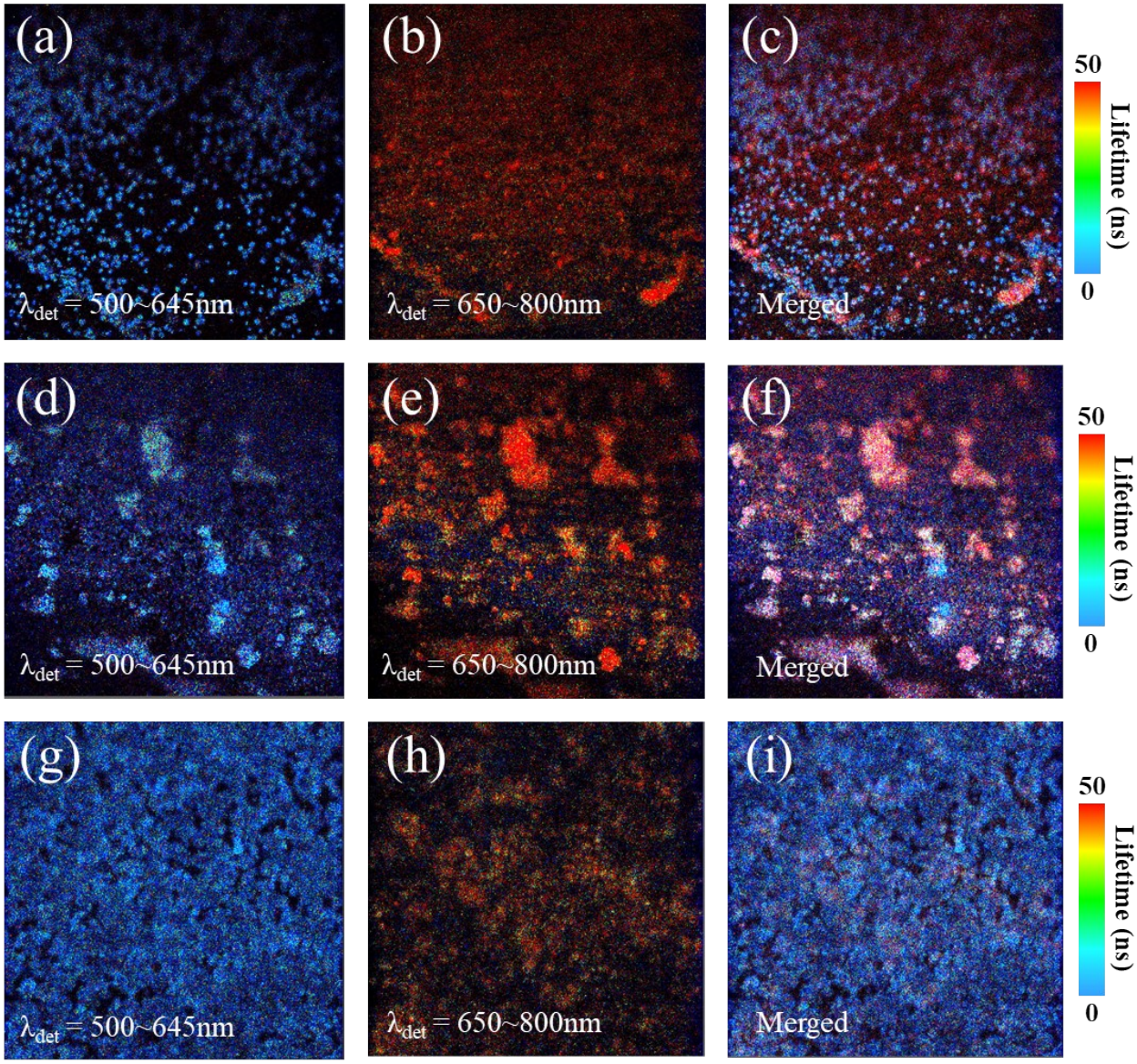

Fig. S12 Photoluminescence lifetime images of the CdSeNS/CdSNR photoanodes reacted for 3, 6, and 12 hr. The PL lifetime imaging was performed at (a,d,g) green-orange (500-645 nm) and (b,e,h) red (650-800 nm) color detections. (c,f, i) Merged images of the two color detections are also presented for comparison.

Table S1. XPS atomic concentrations (at.%) of $CdSe(en)_{0.5}NS/CdSNR$ and CdSeNS/CdSNR-6 photoanode, respectively.

Element	$CdSe(en)_{0.5}NS/CdSNR$-6C	CdSeNS/CdSNR-6
Cd $3d_5$	30.75%	40.81%
Se 3d	23.96%	23.70%
N 1s	22.29%	7.97%
O 1s	23.00%	27.52%
S 2p	0.00%	0.00%
C 1s	0.00%	0.00%

References

1. D. K. Lee, D. Lee, M. A. Lumley and K.-S. Choi, *Chemical Society Reviews*, 2019, **48**, 2126-2157.
2. C. M. Wang, L. W. Lee, T. Y. Chang, B. L. Fan, C. L. Wang, H. M. Lin and K. L. Lu, *Chemistry–A European Journal*, 2016, **22**, 16099-16102.
3. R. P. Patil, M. A. Mahadik, H.-S. Bae, W.-S. Chae, S. H. Choi and J. S. Jang, *Chemical Engineering Journal*, 2020, **402**, 126153.